Protodemetallation Reactions of some Diphenylthallium(III) Compounds with Dicyclohexyldithiophosphinic Acid. Crystal and Molecular Structures of $[TlPh_2\{S_2P(C_6H_{11})_2\}]$, $[TlPh\{S_2P(C_6H_{11})_2\}_2]$ and $[Tl\{S_2P(C_6H_{11})_2\}_3]\cdot CHCl_3$[†]

José S. Casas,[*,a] **Eduardo E. Castellano,**[b] **Alfonso Castiñeiras,**[a] **Agustín Sánchez,**[a]
José Sordo,[a] **Ezequiel M. Vázquez-López**[a] **and Julio Zukerman-Schpector**[b]
[a] *Departamento de Química Inorgánica, Facultade de Farmacia, Universidade de Santiago de Compostela, 15706 Santiago de Compostela, Galicia, Spain*
[b] *Instituto de Física de São Carlos, Universidade de São Paulo, Caixa Postal, 369, CEP 13560 São Carlos, SP, Brazil*

The treatment of diphenylthallium(III) compounds $TlPh_2X$ [X = Br, OH or $S_2P(C_6H_{11})_2$] with dicyclohexyldithiophosphinic acid, $HS(S)P(C_6H_{11})_2$, led to 'protodemetallation' *i.e.* loss of one or more phenyl groups from thallium, with formation of benzene and formation of $[TlPh\{S_2P(C_6H_{11})_2\}_2]$ and $[Tl\{S_2P(C_6H_{11})_2\}_3]\cdot CHCl_3$. The crystal structures of these compounds and that of $[TlPh_2\{S_2P(C_6H_{11})_2\}]$ were solved by X-ray diffraction, which indicated that they all crystallize in the triclinic space group $P\bar{1}$ with $Z = 2$. For $[TlPh_2\{S_2P(C_6H_{11})_2\}]$ $a = 10.141(1)$, $b = 10.315(2)$ and $c = 11.913(2)$ Å, $\alpha = 94.46(1)$, $\beta = 101.45(1)$ and $\gamma = 91.01(1)$°; the thallium atom is co-ordinated to one carbon atom of each phenyl and to both sulfur atoms of a dicyclohexyldithiophosphinate ligand $[S_2P(C_6H_{11})_2]$, and weakly interacts with two neighbouring ligands. For $[TlPh\{S_2P(C_6H_{11})_2\}_2]$ $a = 9.442(1)$, $b = 10.809(2)$ and $c = 18.256(2)$ Å, $\alpha = 80.41(1)$, $\beta = 86.95(1)$ and $\gamma = 72.52(1)$°; the thallium atom is co-ordinated to a phenyl carbon atom and to both sulfur atoms of each anisobidentate $S_2P(C_6H_{11})_2$ ligand. For $[Tl\{S_2P(C_6H_{11})_2\}_3]$ (which incorporates a chloroform solvent molecule) $a = 15.539(1)$, $b = 16.23(3)$ and $c = 10.556(1)$ Å, $\alpha = 103.13(1)$, $\beta = 91.71(1)$ and $\gamma = 111.56(2)$°; the thallium atom is co-ordinated to three pairs of sulfur atoms from two very anisobidentate ligands and one practically isobidentate dithiophosphinate. The IR, Raman, and ^1H, ^{13}C, ^{31}P and ^{205}Tl NMR spectra of the compounds have also been recorded and analysed.

The reaction of some Group 13 or 14 organometallic compounds with dithiophosphorus acids results in their partial 'protodemetallation', *i.e.* the loss of one or more alkyl or aryl groups from the metal, with formation of alkane or arene. For example, treatment of tetraethyllead(IV) with these acids at room temperature results in the cleavage of one, two or three Pb–C bonds and the formation of dithiophosphorus esters of lead;[1] heating them with tetraalkyltin(IV) compounds at 80–100 °C for 5 h leads to trialkylstannyl dithio-phosphates, -phosphonates and -phosphinates;[2] refluxing tetraaryltin(IV) derivatives with diphenyl- and alkenyl-dithiophosphoric acids in 1:1 or 1:2 mole ratio in benzene for *ca.* 4 h affords triaryl- or diaryl-stannyl dithiophosphates;[3] and slow addition of dimethyl- or diphenyl-dithiophosphinic acid to MMe_3 (M = Al, Ga or In) suspended or dissolved in benzene cleaves either one M–C bond (M = Ga or In) or, depending on the acid used and the mole ratio of the reactants, one to three M–C bonds (M = Al), to give the corresponding dithiophosphinates.[4] For organothallium compounds, information regarding protodemetallation reactions is scarce. As well as the disproportionation reaction typical of monoorganothallium derivatives, compounds of the type $PhTlX_2$ (where X = $F_3CCO_2^-$ or $Cl_3CCO_2^-$) are known to undergo protodemetallation reactions with trifluoroacetic acid.[5]

In the course of our studies on the co-ordination of the dithiophosphinate group to organometallic cations, we noted that several diphenylthallium derivatives underwent dephenylation at room temperature in the presence of dicyclohexyldithiophosphinic acid, to afford monophenylthallium(III) dithiophosphinates. This process was easily monitored by ^1H NMR spectroscopy, which confirmed that the monophenyl compound formed was not involved in the equilibrium (1) but

$$2\,[TlPh\{S_2P(C_6H_{11})_2\}_2] \rightleftharpoons [TlPh_2\{S_2P(C_6H_{11})_2\}] + [Tl\{S_2P(C_6H_{11})_2\}_3] \quad (1)$$

was instead stable in solution and isolable. Moreover, the treatment of $HS(S)P(C_6H_{11})_2$ with preformed $[TlPh_2\{S_2P(C_6H_{11})_2\}]$ in a 2:1 mole ratio progressed further until dephenylation was complete and $[Tl\{S_2P(C_6H_{11})_2\}_3]$ formed.

These findings and the crystal structures and spectroscopic properties of $[TlPh_2\{S_2P(C_6H_{11})_2\}]$, $[TlPh\{S_2P(C_6H_{11})_2\}_2]$ and $[Tl\{S_2P(C_6H_{11})_2\}_3]$ are described in this paper. Some synthetic and spectroscopic studies of arylthallium(III) dithiophosphates, dithiocarbamates and dithiocarbonates have been carried out previously, and the structure of *p*-tolylbis(diethyldithiocarbamato)thallium(III) has been reported,[6] but only two diphenylthallium(III) dithiophosphinates have been isolated before and, to our knowledge, there have been no previous X-ray studies of monophenylthallium(III) compounds in which the phenyl rings bears no substituent.

Experimental

Materials and Instrumentation.—The compounds $[NEt_4]Br$, TlBr (Merck) and $HS(S)P(C_6H_{11})_2$ (Strem) were used as

---

[†] *Supplementary data available:* see Instructions for Authors, *J. Chem. Soc., Dalton Trans.*, 1995, Issue 1, pp. xxv–xxx.

supplied and $[NEt_4][S_2P(C_6H_{11})_2]$ was prepared by a published method.[7] Solutions of diphenylthallium(III) hydroxide were obtained by reacting diphenylthallium(III) bromide[8] with a freshly prepared aqueous suspension of Ag_2O. This compound was also prepared by dissolving $TlPh_2Br$ (1.00 g) in refluxing methanol (400 cm^3), mixing in a solution of KOH (1.00 g) in water (20 cm^3) and stirring for 2 d at room temperature (r.t.); after cooling the reaction mixture to 0 °C a white solid formed, which was filtered off, washed with methanol and dried under vacuum.

Elemental analyses were performed with a Carlo Erba 1108 microanalyser. IR spectra of samples in KBr pellets were recorded on a Perkin-Elmer 1330 or a Mattson Cygnus 100 FTIR spectrometer, and Raman spectra of powdered samples in capillary tubes on a Dilor Omars 89 spectrometer (argon-ion laser, $\lambda = 514.5$ nm). All NMR spectra are of solutions in $CDCl_3$; ^1H (250.13), $^{13}C-\{^1H\}$ (62.83) and $^{31}P-\{^1H\}$ (101.26 MHz) spectra were recorded with a Bruker WM 250 NMR spectrometer (at r.t. in 5 mm tubes), and ^{205}Tl and $^{205}Tl-\{^1H\}$ spectra with a Bruker WM 250 spectrometer operating at 144.31 MHz (at 25 ± 0.5 °C in 10 mm tubes). Chemical shifts (δ) in ppm are referred to tetramethylsilane (δ 7.27 for ^1H and 77.0 for ^{13}C NMR spectra), to an external solution of 85% H_3PO_4, or to external $TlClO_4$ extrapolated to infinite dilution.

Preparation of $[TlPh_2\{S_2P(C_6H_{11})_2\}]$.—A solution of $[NEt_4][S_2P(C_6H_{11})_2]$ (0.13 g, 0.33 mmol) in $CHCl_3$ (11 cm^3) was added dropwise to a stirred suspension of $TlPh_2Br$ (0.15 g, 0.34 mmol) in the same solvent (8 cm^3). The solution was stirred further for 1 d before being concentrated *in vacuo*. The residue was treated with ethanol (10 cm^3) and the white precipitate which formed was filtered off, washed with ethanol and dried under vacuum; m.p. 215–217 °C (yield 60%) (Found: C, 46.5; H, 4.8. $C_{24}H_{32}PS_2Tl$ requires C, 46.5; H, 5.2%). Single crystals of this compound suitable for X-ray diffraction measurements were obtained in the protodemetallation reactions (see below).

Protodemetallation Reactions.—(*i*) $TlPh_2OH$ *and* $HS(S)P(C_6H_{11})_2$. In an NMR tube, solid $TlPh_2OH$ (12.0 mg, 0.032 mmol) was shaken with a solution of $HS(S)P(C_6H_{11})_2$ (11.3 mg, 0.043 mmol) in $CDCl_3$ (0.6 cm^3) until it dissolved, and the ^1H NMR spectrum of the solution was immediately recorded. This showed signals due to mono- and di-phenylated Tl^{III} species and a sharp singlet at δ 7.37 which was attributed to benzene formed in the protodemetallation reaction; monitoring for several days showed no changes. The $CDCl_3$ was slowly evaporated to afford a crystalline product, $[TlPh_2\{S_2P(C_6H_{11})_2\}]$, a single crystal of which was used for a crystal structure determination as described below.

A larger scale reaction was carried out using $TlPh_2OH$ prepared *in situ* by mixing $TlPh_2Br$ (0.87 g, 2.28 mmol) and Ag_2O (0.68 g, 2.94 mmol) in water (30 cm^3). Treatment of this solution with $HS(S)P(C_6H_{11})_2$ (0.60 g, 2.29 mmol) in ethanol (50 cm^3) afforded a very pale yellow precipitate, which was filtered off and dried over $CaCl_2$ in a vacuum desiccator. Elemental analysis of this product suggested that it was a mixture. Extraction of 0.20 g of this crude material with $CHCl_3$ (10 cm^3), followed by quick filtration of the extracts and evaporation of the solvent *in vacuo*, afforded a solid which was identified by elemental analysis and an ^1H NMR spectrum as $[TlPh\{S_2P(C_6H_{11})_2\}_2]$; m.p. 188–190 °C (yield 35%) (Found: C, 44.7; H, 6.2. $C_{30}H_{49}P_2S_4Tl$ requires C, 43.2; H, 6.4%). (For selected NMR spectroscopic data see Table 9.)

(*ii*) $TlPh_2Br$ *and* $HS(S)P(C_6H_{11})_2$. A solution of $HS(S)P(C_6H_{11})_2$ (0.09 g, 0.34 mmol) dissolved in $CHCl_3$ (8 cm^3) was added slowly and with stirring to $TlPh_2Br$ (0.15 g, 0.34 mmol) dissolved in dimethylformamide (dmf). The solution was stirred for 2 d, concentrated *in vacuo* to half its initial volume, filtered and stored at 0 °C. After two days a crystalline white product formed which was isolated and characterized by ^1H, $^{13}C-\{^1H\}$, $^{31}P-\{^1H\}$ and $^{205}Tl-\{^1H\}$ NMR spectroscopy, which indicated the structure $[TlPh\{S_2P(C_6H_{11})_2\}_2]$ (see Table 9). Single crystals of this material suitable for X-ray analysis were obtained by recrystallization from chloroform.

(*iii*) $[TlPh_2\{S_2P(C_6H_{11})_2\}]$ *and* $HS(S)P(C_6H_{11})_2$. Four equal portions of $HS(S)P(C_6H_{11})_2$ (7.1 mg, 0.027 mmol each) were added slowly and with shaking to $[TlPh_2\{S_2P(C_6H_{11})_2\}]$ (33.7 mg, 0.054 mmol) dissolved in $CDCl_3$ (2.5 cm^3). After each addition ^1H and ^{205}Tl NMR spectra of the reaction mixture were recorded, and after the final spectrum (at 2:1 mole ratio) the solution was stored for several days. Yellow-orange crystals of $[Tl\{S_2P(C_6H_{11})_2\}_3]\cdot CHCl_3$ formed, which were used for X-ray diffraction and NMR spectroscopic studies.

Crystal Structure Determinations.—X-Ray diffraction studies of the complexes $[TlPh_2\{S_2P(C_6H_{11})_2\}]$, $[TlPh\{S_2P(C_6H_{11})_2\}_2]$ and $[Tl\{S_2P(C_6H_{11})_2\}_3]\cdot CHCl_3$ were performed with an Enraf-Nonius CAD-4 diffractometer. Crystal data and experimental conditions are given in Table 1.

The structures of $[TlPh_2\{S_2P(C_6H_{11})_2\}]$ and $[TlPh\{S_2P(C_6H_{11})_2\}_2]$ were solved using the Patterson method, and that of $[Tl\{S_2P(C_6H_{11})_2\}_3]\cdot CHCl_3$ by direct methods. Fourier-difference maps enabled all the non-hydrogen atoms to be located. All the non-hydrogen atoms were refined with anisotropic thermal parameters. For $[TlPh\{S_2P(C_6H_{11})_2\}_2]$ and $[Tl\{S_2P(C_6H_{11})_2\}_3]\cdot CHCl_3$, H atoms were included in calculated positions in the structure calculations but were not refined. Empirical absorption corrections were applied.[9] Calculations were performed using the programs SHELXS[10] and VAXSDP,[11] and graphical representations by ORTEP[12] and SCHAKAL.[13] For the two organometallic complexes scattering factors and anomalous dispersion corrections were taken from refs. 14 and 15, respectively, while for $[Tl\{S_2P(C_6H_{11})_2\}_3]\cdot CHCl_3$ they were obtained from ref. 16.

Additional material available from the Cambridge Crystallographic Data Centre comprises calculated H-atom coordinates, thermal parameters and remaining bond distances and angles.

Results and Discussion

Reactions of $TlPh_2Br$ *with* $[S_2P(C_6H_{11})_2]^-$ *and* $TlPh_2X$ *with* $HS(S)P(C_6H_{11})_2$ [X = OH, Br *or* $S_2P(C_6H_{11})_2$].—The reaction between diphenylthallium(III) bromide and ammonium dicyclohexyldithiophosphinate is a straightforward metathetical reaction giving the organometallic dithiophosphinate $[TlPh_2\{S_2P(C_6H_{11})_2\}]$ and ammonium bromide.

Mixtures of $TlPh_2X$ [X = OH, Br or $S_2P(C_6H_{11})_2$] and $HS(S)P(C_6H_{11})_2$ in different solvents underwent protodemetallation reactions which gave the complexes $[TlPh\{S_2P(C_6H_{11})_2\}_2]$ and $[Tl\{S_2P(C_6H_{11})_2\}_3]$. The influence of the mole ratio of the reactants on product composition was explored by ^1H and ^{205}Tl NMR spectroscopy, chiefly for mixtures of $[TlPh_2\{S_2P(C_6H_{11})_2\}]$ and $HS(S)P(C_6H_{11})_2$, see Fig. 1. The signals corresponding to mono- and di-phenylthallium(III) derivatives are easily distinguished by examination of the coupling between *ortho*-, *meta*- or *para*-phenyl protons and the Tl nucleus, which is considerably stronger for monophenyl compounds (*e.g.* see ref. 17). Fig. 1(*a*) shows part of the ^1H NMR spectrum of $[TlPh_2\{S_2P(C_6H_{11})_2\}]$ in $CDCl_3$, and the changes induced upon the addition of $HS(S)P(C_6H_{11})_2$. Compared to the spectrum obtained for a diphenylthallium(III) dithiophosphinate–acid mole ratio of 1:0, that for a mole ratio of 1:0.5 shows additional signals due to the monophenyl derivative and a very sharp signal due to benzene, both of which are formed in the protodemetallation reaction; integration of the signals due to the organometallic moieties indicates that the concentrations of $[TlPh_2\{S_2P(C_6H_{11})_2\}]$ and $[TlPh\{S_2P(C_6H_{11})_2\}_2]$ are practically the same under the experimental conditions employed. The signals due to the diphenyl derivative disappear completely when the mole ratio of the reactants is 1:1 and only the signals due to monophenylthallium(III) are seen in the high frequency range of the spectrum.

Table 1 Crystallographic data[a]

	$[TlPh_2\{S_2P(C_6H_{11})_2\}]$	$[TlPh\{S_2P(C_6H_{11})_2\}_2]$	$[Tl\{S_2P(C_6H_{11})_2\}_3]\cdot CHCl_3$
Molecular formula	$C_{24}H_{32}PS_2Tl$	$C_{30}H_{49}P_2S_4Tl$	$C_{37}H_{67}P_3S_6Cl_3Tl$
M	619.99	804.80	1107.98
a/Å	10.141(1)	9.442(1)	15.539(1)
b/Å	10.315(2)	10.809(2)	16.23(3)
c/Å	11.913(2)	18.256(2)	10.556(1)
α/°	94.46(1)	80.41(1)	103.13(1)
β/°	101.45(1)	86.95(1)	91.71(1)
γ/°	91.01(1)	72.52(1)	111.56(2)
U/Å^3	1219.9(6)	1752.3(5)	2392.2(5)
D_c/g cm^{-3}	1.69	1.52	1.54
F(000)	608	808	1124
Crystal dimensions/mm	0.30–0.30	0.25–0.05	0.30 × 0.25 × 0.20
h,k,l Range	−12 to 11; −12 to 12; 0–14	−10 to 10; −11 to 11; 0–20	−21 to 21; −22 to 22; −14 to 14
Maximum, minimum transmission factors	0.87, 1.69	0.70, 1.53	0.49, 1.21
Maximum, minimum residual electron density/e Å^{-3}	−1.4, 2.7	−1.0, 1.7	−0.7, 1.7
μ(Mo-Kα)/cm^{-1}	62.25	49.92	39.56
Scan technique	ω–2θ	ω–2θ	ω–2θ
θ Range/°	0–25	0–23	3–30
Reflections measured	4165	3538	13 918
Reflections above 3$\sigma(I)$	3141	3168	6771
x in $w^{-1} = \sigma^2(F) + x(F)^2$	0.0012	0.0002	0
R[b]	0.050	0.049	0.052
R′[c]	0.052	0.051	0.056

[a] Details in common: triclinic, space group $P\bar{1}$, $Z = 2$, $T = 293$ K, λ(Mo-Kα) = 0.710 73 Å. [b] $R = \Sigma(|F_o| - |F_c|)/\Sigma|F_o|$. [c] $R' = [\Sigma(|F_o| - |F_c|)^2/\Sigma w|F_o|^2]^{\frac{1}{2}}$.

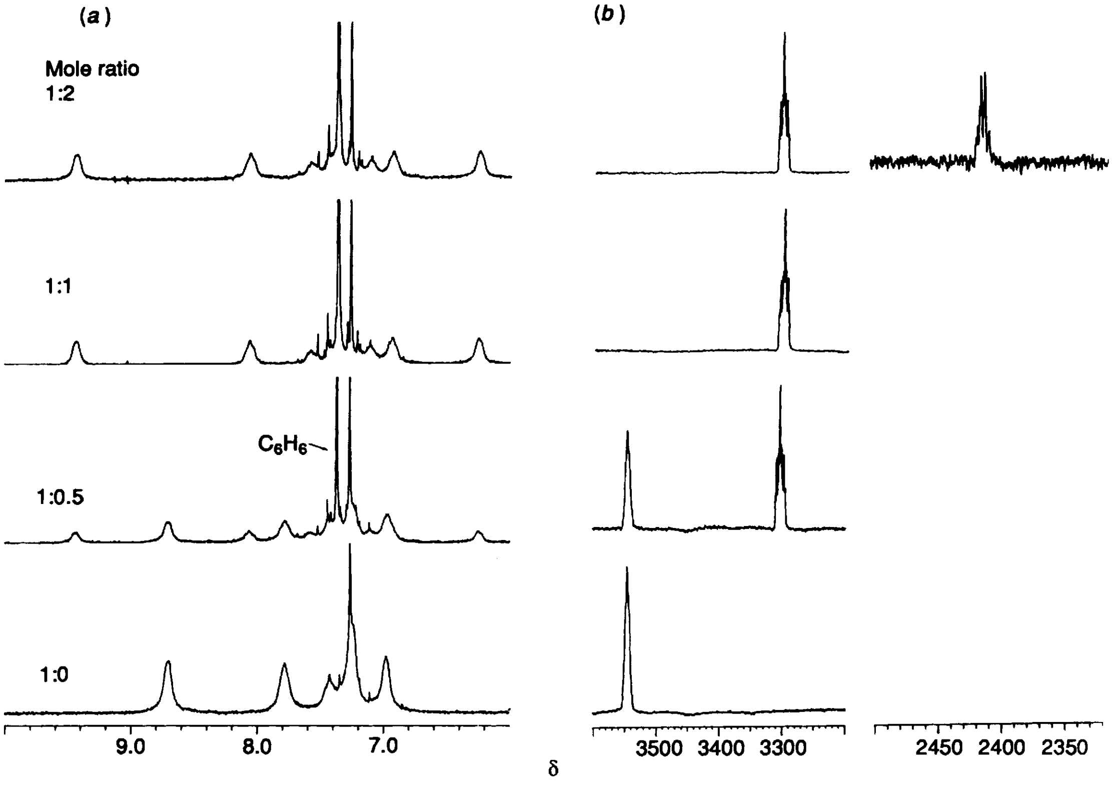

Fig. 1 (*a*) ^1H, (*b*) ^{205}Tl NMR spectra in $CDCl_3$ of mixtures of $[TlPh_2\{S_2P(C_6H_{11})_2\}]$ and $HS(S)P(C_6H_{11})_2$ at varying mole ratios

The ^{205}Tl NMR spectroscopic studies confirm these results [Fig. (1*b*)]. In the proton-coupled spectrum of $[TlPh_2\{S_2P(C_6H_{11})_2\}]$ only one signal is seen, while two are visible at a 1 : 0.5 mole ratio of reactants, the lower frequency signal (which has the stronger thallium–proton coupling) being associated with the monophenyl derivative formed by partial protodemetallation of the diphenylthallium(III) species. The higher frequency signal does not appear at a 1 : 1 mole ratio, indicating that protodemetallation proceeds until the reaction is complete, equation (2).

$$[TlPh_2\{S_2P(C_6H_{11})_2\}] + HS(S)P(C_6H_{11})_2 \longrightarrow [TlPh\{S_2P(C_6H_{11})_2\}_2] + C_6H_6 \quad (2)$$

Interestingly, the spectrum for a 1 : 2 mole ratio of reactants shows both the monophenylthallium(III) signal and a signal

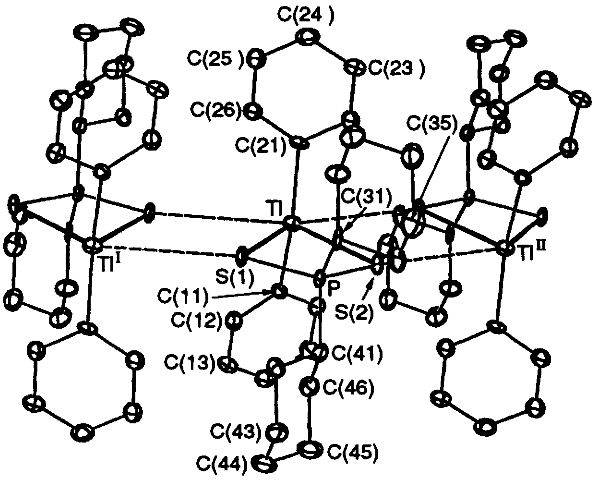

Fig. 2 An ORTEP drawing showing the intermolecular interactions along the *b* axis in $[TlPh_2\{S_2P(C_2P(C_6H_{11})_2\}]$ and the atom numbering scheme

Table 2 Fractional atomic coordinates for $[TlPh_2\{S_2P(C_6H_{11})_2\}]$

Atom	*x*	*y*	*z*
Tl	−0.0702(1)	0.2495(1)	0.0016(1)
S(1)	0.1481(3)	0.0889(2)	0.0025(2)
S(2)	0.1516(3)	0.4109(2)	−0.0119(2)
P	0.2614(2)	0.2501(2)	−0.0042(2)
C(11)	−0.1550(9)	0.227(1)	−0.1763(8)
C(12)	−0.147(1)	0.109(1)	−0.240(1)
C(13)	−0.201(1)	0.097(1)	−0.359(1)
C(14)	−0.259(1)	0.199(1)	−0.413(1)
C(15)	−0.267(1)	0.318(1)	−0.351(1)
C(16)	−0.217(1)	0.332(1)	−0.232(1)
C(21)	−0.055(1)	0.270(1)	0.1810(8)
C(22)	−0.007(1)	0.388(1)	0.246(1)
C(23)	0.011(1)	0.399(1)	0.366(1)
C(24)	−0.016(1)	0.291(1)	0.422(1)
C(25)	−0.060(1)	0.174(1)	0.361(1)
C(26)	−0.081(1)	0.165(1)	0.241(1)
C(31)	0.400(1)	0.2671(9)	0.1236(9)
C(32)	0.340(1)	0.284(1)	0.233(1)
C(33)	0.454(2)	0.296(2)	0.341(1)
C(34)	0.555(1)	0.406(1)	0.334(1)
C(35)	0.612(1)	0.391(2)	0.224(1)
C(36)	0.498(1)	0.380(1)	0.115(1)
C(41)	0.338(1)	0.231(1)	−0.1308(9)
C(42)	0.430(1)	0.112(1)	−0.126(1)
C(43)	0.496(1)	0.098(1)	−0.232(1)
C(44)	0.358(1)	0.085(2)	−0.343(1)
C(45)	0.300(1)	0.207(2)	−0.349(1)
C(46)	0.231(1)	0.223(1)	−0.242(1)

split by thallium–phosphorus coupling $[^2J(^{205}Tl{-}^{31}P) = 439.4$ Hz, see Fig. 1(*b*)]. This is attributed to the fully dephenylated thallium(III) dithiophosphinate $[Tl\{S_2P(C_6H_{11})_2\}_3]$, which is formed by reaction (3).

$$[TlPh\{S_2P(C_6H_{11})_2\}_2] + HS(S)P(C_6H_{11})_2 \longrightarrow [Tl\{S_2P(C_6H_{11})_2\}_3] + C_6H_6 \quad (3)$$

In this case the reaction does not reach completion, although crystals of the new complex were obtained after storing the solution for several days. Note that the formation of this product is in sharp contrast to the formation of $[Tl(S_2PEt_2)]$ by the direct reaction (4) between Tl^{III} and diethyldithiophosphinate anion.[18,19]

$$Tl^{3+} + 3\ Et_2PS_2^- \longrightarrow [Tl(S_2PEt_2)] + (S_2PEt_2)_2 \quad (4)$$

Table 3 Selected interatomic distances (Å) and angles (°) in $[TlPh_2\{S_2P(C_6H_{11})_2\}]$, with estimated standard deviations (e.s.d.s) in parentheses *

Tl–S(1)	2.789(3)	Tl–S(2^{II})	3.614(3)
Tl–S(2)	2.816(3)	S(1)–P	2.022(4)
Tl–C(11)	2.117(9)	S(2)–P	2.013(4)
Tl–C(21)	2.107(9)	P–C(31)	1.85(1)
Tl–S(1^{I})	3.563(3)	P–C(41)	1.83(1)
S(1)–Tl–S(2)	73.19(8)	S(2^{II})–Tl–S(1^{I})	153.69(6)
S(1)–Tl–C(11)	98.7(3)	Tl–S(1)–P	87.8(1)
S(1)–Tl–C(21)	96.4(3)	Tl–S(1)–Tl^{I}	114.80(8)
C(11)–Tl–C(21)	160.6(4)	P–S(1)–Tl^{I}	157.2(1)
S(1)–Tl–S(2^{II})	141.05(7)	Tl–S(2)–P	87.2(1)
S(1)–Tl–S(1^{I})	65.20(7)	Tl–S(2)–Tl^{II}	111.89(8)
S(2)–Tl–C(11)	97.2(3)	P–S(1)–Tl^{II}	160.1(1)
S(2)–Tl–C(21)	98.6(3)	S(1)–P–S(2)	111.8(2)
S(2)–Tl–S(2^{II})	68.11(7)	S(1)–P–C(31)	109.0(3)
S(2)–Tl–S(1^{I})	138.17(7)	S(1)–P–C(41)	109.3(4)
C(11)–Tl–S(2^{II})	90.4(3)	S(2)–P–C(31)	110.2(3)
C(11)–Tl–(S(1^{I})	85.3(3)	S(2)–P–C(41)	109.1(4)
C(21)–Tl–S(2^{II})	85.3(3)	C(31)–P–C(41)	107.3(5)
C(21)–Tl–S(1^{I})	90.2(3)		

* Symmetry codes: I $-x, -y, -z$; II $-x, 1 - y, -z$.

Structure of $[TlPh_2\{S_2P(C_6H_{11})_2\}]$.—The structure of $[TlPh_2\{S_2P(C_6H_{11})_2\}]$ and the atom numbering scheme used is shown in Fig. 2, the fractional atomic coordinates are listed in Table 2, and selected bond distances and bond angles in Table 3.

The thallium atom is co-ordinated to two sulfur atoms of a practically isobidentate dithiophosphinate ligand. The P–S bond distances are typical of this ligand,[20] and the Tl–C and Tl–S distances are also unexceptional, being similar to those found in $[TlPh_2(S_2CNEt_2)]$ (although the C–Tl–C angle is slightly wider in the dithiocarbamate).[21] While in the latter compound only one secondary intermolecular interaction was observed, in the dithiophosphinate there are at least two possible weak Tl–S interactions, although in both cases the interatomic distances are very close to the sum of the van der Waals radii (3.75 Å).[22] These interactions involve Tl and two S atoms (one from each of two neighbouring molecules), and connect the chelate rings in infinite chains running parallel to the *b* axis (Fig. 2). If these weak interactions are taken into account, each thallium atom has very distorted octahedral co-ordination geometry, with the phenyl carbon and sulfur atoms in apical and equatorial positions respectively.

Structure of $[TlPh\{S_2P(C_6H_{11})_2\}_2]$.—To our knowledge, this is the first X-ray study of monophenylthallium(III) compound in which the phenyl ring bears no substituent, although the crystal structure of $[Tl(C_6H_4Me\text{-}p)(S_2CNEt_2)_2]$ has been reported.[6] The structure of $[TlPh\{S_2P(C_6H_{11})_2\}_2]$ is shown in Fig. 3, and fractional atomic coordinates and selected bond distances and bond angles are listed in Tables 4 and 5, respectively.

The crystal structure comprises discrete molecules in which the thallium atom is co-ordinated to the four sulfur atoms of two anisobidentate dicyclohexyldithiophosphinate ligands and to a carbon atom of the phenyl group. The Tl–S and Tl–C distances are close to those found in $[Tl(C_6H_4Me\text{-}p)(S_2CNEt_2)_2]$, although the dithiophosphinates are more anisobidentate than the diethyldithiocarbamate ligands. The anisobidenticity of the ligands is also reflected in the P–S distances, S atoms involved in short Tl–S bonds forming long P–S bonds, and *vice versa* (see Table 5). The average Tl–S bonds are shorter than in the diphenylthallium dithiophosphinate complex (see above), which suggests reinforcement of the Tl–S bonds due to the increase in charge of the organometallic cation. There are no intermolecular interactions.

Table 4 Fractional atomic coordinates for [TlPh{$S_2P(C_6H_{11})_2$}$_2$]

Atom	*x*	*y*	*z*
Tl	0.2780(1)	0.2056(1)	0.2372(1)
C(1)	0.354(2)	0.030(2)	0.1892(8)
C(2)	0.349(2)	0.032(2)	0.1151(8)
C(3)	0.392(2)	−0.083(2)	0.0837(9)
C(4)	0.433(2)	−0.198(2)	0.126(1)
C(5)	0.418(3)	−0.208(2)	0.206(1)
C(6)	0.379(2)	−0.094(2)	0.2386(9)
P(1)	0.0010(3)	0.4437(3)	0.1574(2)
S(11)	0.1949(3)	0.3941(3)	0.1038(2)
S(12)	0.0142(4)	0.3417(4)	0.2626(2)
C(111)	−0.145(1)	0.414(1)	0.1064(6)
C(112)	−0.105(2)	0.269(1)	0.0975(8)
C(113)	−0.227(2)	0.250(2)	0.0521(8)
C(114)	−0.380(2)	0.297(2)	0.0857(8)
C(115)	−0.413(2)	0.434(1)	0.0992(8)
C(116)	−0.296(2)	0.458(1)	0.1448(7)
C(121)	−0.061(2)	0.619(1)	0.1656(7)
C(122)	−0.092(2)	0.704(1)	0.0889(8)
C(123)	−0.140(2)	0.849(2)	0.971(1)
C(124)	−0.025(3)	0.882(2)	0.137(2)
C(125)	0.010(3)	0.801(2)	0.209(1)
C(126)	0.060(2)	0.656(2)	0.2040(8)
P(2)	0.4494(4)	0.2225(3)	0.3844(2)
S(21)	0.4399(4)	0.3301(4)	0.2804(2)
S(22)	0.3198(4)	0.1064(4)	0.3925(2)
C(211)	0.643(1)	0.128(1)	0.4043(7)
C(212)	0.698(2)	0.020(1)	0.3573(8)
C(213)	0.861(2)	−0.062(2)	0.3822(8)
C(214)	0.958(2)	0.027(2)	0.3749(9)
C(215)	0.903(2)	0.135(2)	0.4193(9)
C(216)	0.744(2)	0.216(1)	0.3984(7)
C(221)	0.393(2)	0.339(1)	0.4516(7)
C(222)	0.240(2)	0.427(2)	0.4360(9)
C(223)	0.198(2)	0.523(2)	0.491(1)
C(224)	0.213(2)	0.455(2)	0.570(1)
C(225)	0.367(2)	0.366(2)	0.5857(8)
C(226)	0.412(2)	0.271(2)	0.5301(8)

Table 5 Selected interatomic distances (Å) and angles (°) in [TlPh{$S_2P(C_6H_{11})_2$}$_2$] with e.s.d.s in parentheses

Tl–C(1)	2.13(2)	P(1)–C(111)	1.84(1)
Tl–S(11)	2.879(3)	P(1)–C(121)	1.84(1)
Tl–S(12)	2.547(4)	P(2)–S(21)	2.046(5)
Tl–S(21)	2.547(4)	P(2)–S(22)	1.984(5)
Tl–S(22)	2.863(3)	P(2)–C(211)	1.83(1)
P(1)–S(11)	1.998(5)	P(2)–C(221)	1.85(1)
P(1)–S(12)	2.039(4)		
C(1)–Tl–S(11)	99.3(4)	S(12)–P(1)–C(111)	109.3(4)
C(1)–Tl–S(12)	129.8(4)	S(12)–P(1)–C(121)	106.9(5)
C(1)–Tl–S(21)	126.3(4)	C(111)–P(1)–C(121)	106.4(6)
C(1)–Tl–S(22)	102.0(4)	Tl–S(11)–P(1)	82.1(1)
S(11)–Tl–S(12)	75.7(1)	Tl–S(12)–P(1)	90.3(2)
S(11)–Tl–S(21)	92.1(1)	S(21)–P(2)–S(22)	111.3(2)
S(11)–Tl–S(22)	158.7(1)	S(21)–P(2)–C(211)	108.2(5)
S(12)–Tl–S(21)	103.9(1)	S(21)–P(2)–C(221)	107.7(5)
S(12)–Tl–S(22)	90.2(1)	S(22)–P(2)–C(211)	111.4(5)
S(21)–Tl–S(22)	75.7(1)	S(22)–P(2)–C(221)	111.1(5)
S(11)–P(1)–S(12)	111.6(2)	C(211)–P(2)–C(221)	106.9(6)
S(11)–P(1)–C(111)	110.4(4)	Tl–S(21)–P(2)	90.0(2)
S(11)–P(1)–C(121)	112.0(5)	Tl–S(22)–P(2)	82.7(2)

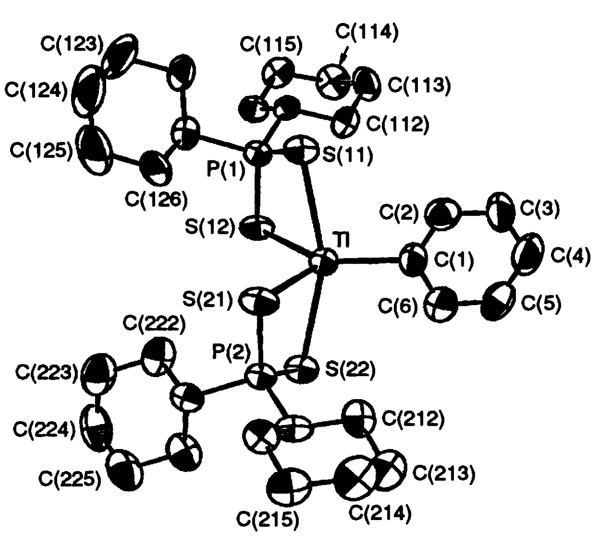

Fig. 3 An ORTEP drawing showing the molecular structure of [TlPh{$S_2P(C_6H_{11})_2$}$_2$] and the atom numbering scheme

The bond angles suggest a co-ordination polyhedron closer to a trigonal bipyramid than a square pyramid. The S(11) and S(22) atoms occupy the apical positions, although the S(11)–Tl–S(22) angle [158.7(1)°] differs widely from the ideal value of 180°, probably because of the bite of the ligand.

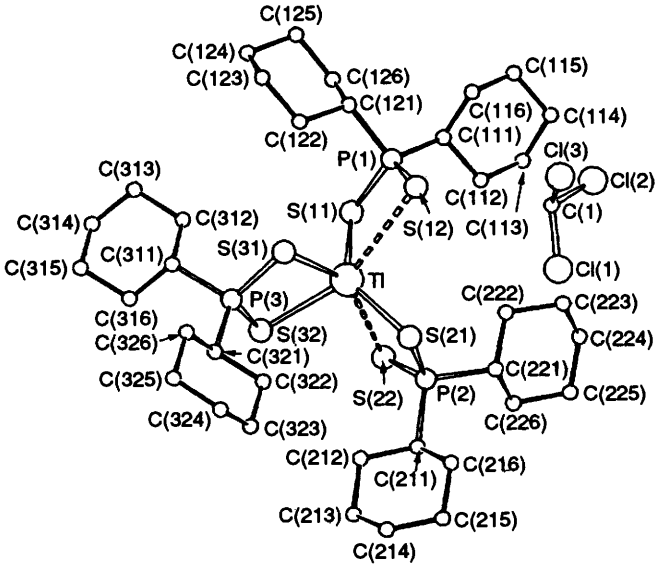

Fig. 4 A SCHAKAL drawing showing the molecular structure of [Tl{$S_2P(C_6H_{11})_2$}$_3$]·$CHCl_3$ and the atom numbering scheme

Structure of [Tl{$S_2P(C_6H_{11})_2$}$_3$]·$CHCl_3$.—The structure and atom numbering scheme of [Tl{$S_2P(C_6H_{11})_2$}$_3$]·$CHCl_3$ are shown in Fig. 4, and fractional atomic coordinates and selected bond distances and angles are listed in Tables 6 and 7, respectively.

The complex crystallized from $CHCl_3$ with one solvent molecule. The three dithiophosphinate ligands show two different modes of co-ordination: those containing the P(1) and P(2) atoms are very anisobidentate, with one Tl–S bond distance *ca.* 2.4 (the shortest yet seen in a Tl^{III} dithioligand complex); and the other > 3.1 Å, while the ligand containing P(3) is practically isobidentate, with Tl–S distances close to those found in [Tl(S_2CNMe_2)$_3$].[23] In the anisobidentate ligands, the S atoms in long Tl–S bonds are involved in short P–S bonds and *vice versa* (see Table 7), as observed in the monophenylthallium(III) compound, while in the isobidentate ligand the P–S distances are, as expected, similar [P(3)–S(31) 2.022(3) and P(3)–S(32) 2.026(3) Å].

The structural features of this complex are very different from

Table 6 Fractional atomic coordinates for $[\mathrm{Tl}\{\mathrm{S_2P(C_6H_{11})_2}\}_3]\cdot\mathrm{CHCl_3}$

Atom	*x*	*y*	*z*
Tl	0.196 78(3)	0.785 49(2)	0.220 90(4)
Cl(1)	0.553 1(4)	0.742 7(4)	0.123 7(5)
Cl(2)	0.485 9(4)	0.585 2(3)	−0.085 6(7)
Cl(3)	0.575 3(4)	0.759 1(4)	−0.132 8(5)
S(11)	0.083 8(2)	0.640 3(2)	0.077 8(2)
S(12)	0.285 1(2)	0.733 0(2)	−0.042 4(2)
S(21)	0.355 0(2)	0.836 9(2)	0.338 8(2)
S(22)	0.176 2(2)	0.686 5(2)	0.444 5(2)
S(31)	0.202 8(2)	0.927 5(1)	0.129 5(2)
S(32)	0.092 7(2)	0.853 9(2)	0.372 1(2)
P(1)	0.157 9(2)	0.637 0(1)	−0.082 7(2)
P(2)	0.312 9(2)	0.754 5(2)	0.467 8(2)
P(3)	0.124 3(1)	0.951 6(1)	0.271 6(2)
C(1)	0.504 8(7)	0.697 1(8)	−0.034(1)
C(111)	0.154 5(6)	0.519 6(5)	−0.128 6(8)
C(112)	0.205 1(7)	0.499 7(6)	−0.020(1)
C(113)	0.198 6(8)	0.400 8(7)	−0.061(1)
C(114)	0.233 8(8)	0.379 1(7)	−0.191(1)
C(115)	0.187 0(8)	0.402 0(7)	−0.297(1)
C(116)	0.194 6(7)	0.501 9(6)	−0.259(1)
C(121)	0.087 8(5)	0.648 5(5)	−0.217 7(8)
C(122)	0.077 5(7)	0.740 4(6)	−0.179 8(9)
C(123)	0.020 1(7)	0.752 3(6)	−0.289(1)
C(124)	−0.073 9(7)	0.674 0(8)	−0.327(1)
C(125)	−0.061 5(7)	0.582 1(7)	−0.369(1)
C(126)	−0.006 0(7)	0.569 6(7)	−0.259(1)
C(211)	0.359 5(6)	0.830 7(6)	0.633 6(8)
C(212)	0.310 7(6)	0.897 8(7)	0.668(1)
C(213)	0.347 8(7)	0.959 0(7)	0.808(1)
C(214)	0.453 2(8)	1.010 5(7)	0.822(1)
C(215)	0.500 9(8)	0.944 0(8)	0.789(1)
C(216)	0.465 0(6)	0.881 0(7)	0.651(1)
C(221)	0.374 8(6)	0.676 0(5)	0.436 8(9)
C(222)	0.344 5(7)	0.615 0(7)	0.297 4(9)
C(223)	0.391 2(8)	0.546 0(7)	0.271(1)
C(224)	0.370 0(7)	0.487 9(7)	0.370(1)
C(225)	0.402 6(7)	0.548 3(7)	0.507(1)
C(226)	0.357 8(7)	0.619 5(6)	0.538 7(9)
C(311)	0.016 9(5)	0.953 8(5)	0.198 2(8)
C(312)	−0.039 5(7)	0.862 6(7)	0.099(1)
C(313)	−0.127 8(7)	0.863 1(7)	0.036(1)
C(314)	−0.187 0(7)	0.887 7(7)	0.138(1)
C(315)	−0.131 7(7)	0.978 6(7)	0.236(1)
C(316)	−0.042 5(6)	0.978 7(6)	0.300 6(9)
C(321)	0.187 1(6)	1.063 7(5)	0.387 4(8)
C(322)	0.279 0(6)	1.067 9(6)	0.448 0(9)
C(323)	0.331 7(7)	1.159 0(7)	0.549(1)
C(324)	0.345 5(7)	1.239 1(7)	0.492(1)
C(325)	0.254 9(7)	1.233 6(7)	0.426(1)
C(326)	0.204 1(6)	1.143 3(6)	0.323 5(9)

Table 7 Selected interatomic distances (Å) and angles (°) in $[\mathrm{Tl}\{\mathrm{S_2P(C_6H_{11})_2}\}_3]\cdot\mathrm{CHCl_3}$ with e.s.d.s in parentheses

Tl–S(11)	2.471(2)	S(22)–P(2)	1.977(3)
Tl–S(12)	3.217(2)	S(31)–P(3)	2.022(3)
Tl–S(21)	2.475(2)	S(32)–P(3)	2.026(3)
Tl–S(22)	3.107(3)	P(1)–C(111)	1.836(9)
Tl–S(31)	2.667(3)	P(1)–C(121)	1.85(1)
Tl–S(32)	2.658(3)	P(2)–C(211)	1.843(8)
S(11)–P(1)	2.078(3)	P(2)–C(221)	1.84(2)
S(12)–P(1)	1.975(3)	P(3)–C(311)	1.834(9)
S(21)–P(2)	2.075(4)	P(3)–C(321)	1.836(7)
S(11)–Tl–S(12)	71.12(7)	S(11)–P(1)–C(121)	106.6(3)
S(11)–Tl–S(21)	135.59(9)	S(12)–P(1)–C(111)	114.2(3)
S(11)–Tl–S(22)	87.85(7)	S(12)–P(1)–C(121)	112.4(3)
S(11)–Tl–S(31)	110.82(8)	C(111)–P(1)–C(121)	106.8(4)
S(11)–Tl–S(32)	104.34(8)	S(21)–P(2)–S(22)	112.5(2)
S(12)–Tl–S(21)	86.60(7)	S(21)–P(2)–C(211)	106.1(4)
S(12)–Tl–S(22)	124.11(7)	S(21)–P(2)–C(221)	105.8(3)
S(12)–Tl–S(31)	83.09(8)	S(22)–P(2)–C(211)	113.5(4)
S(12)–Tl–S(32)	156.78(8)	S(22)–P(2)–C(221)	111.3(3)
S(21)–Tl–S(22)	73.30(7)	C(211)–P(2)–C(221)	107.0(4)
S(21)–Tl–S(31)	103.69(8)	S(31)–P(3)–C(32)	110.6(2)
S(21)–Tl–S(32)	109.94(7)	S(31)–P(3)–C(311)	109.6(3)
S(22)–Tl–S(31)	151.68(7)	S(31)–P(3)–C(321)	110.6(3)
S(22)–Tl–S(32)	77.48(8)	S(32)–P(3)–C(311)	110.0(3)
S(31)–Tl–S(32)	77.33(8)	S(32)–P(3)–C(321)	108.5(3)
S(11)–P(1)–S(12)	112.0(1)	C(311)–P(3)–C(321)	107.5(5)
S(11)–P(1)–C(111)	104.3(3)		

Table 8 Selected IR and Raman bands (cm^{-1})[a]

	ν(PS)		
Compound	ν_{asym}	ν_{sym}	$\Delta\nu$[b]
$[\mathrm{NEt_4}][\mathrm{S_2P(C_6H_{11})_2}]$	620vs	555s	65
	(—)	(551s)[c]	
$\mathrm{HS(S)P(C_6H_{11})_2}$	630vs	520s	110
	(—)	(525s)	
$[\mathrm{TlPh_2}\{\mathrm{S_2P(C_6H_{11})_2}\}]$	595vs	545s	40
	(—)	(550s)	
$[\mathrm{TlPh}\{\mathrm{S_2P(C_6H_{11})_2}\}_2]$	605s	545s	85
	(601w)	(548w)	
$[\mathrm{Tl}\{\mathrm{S_2P(C_6H_{11})_2}\}_3]\cdot\mathrm{CHCl_3}$	621s (br)	528vs (br)	93

[a] br = Broad, s = strong, vs = very strong, w = weak. [b] $\Delta\nu = \nu_{asym} - \nu_{sym}$. [c] Raman data in parentheses.

those of the Tl^{I} dithiophosphinate $[\mathrm{Tl(S_2PEt_2)}]$.[19] In the latter compound, even the Tl–S bonds forming the symmetric chelate ring are very long [3.056(7) Å], which is attributed to the bridging nature of the S atoms and largely ionic bonding (each S is involved in additional weak interactions with the Tl^{I} atoms of four adjacent molecules). Thallium(III) is a better electron acceptor, so leading to some stronger and more covalent Tl–S bonds.

Vibrational Spectra.—Selected IR and Raman vibrational bands characteristic of the complexes are listed in Table 8, which also includes data for $[\mathrm{NEt_4}][\mathrm{S_2P(C_6H_{11})_2}]$ and $\mathrm{HS(S)P(C_6H_{11})_2}$ for comparison. The parameter $\Delta\nu$ [= ν_{asym}(P–S) − ν_{sym}(P–S)] has been proposed[24] as indicative of the mode of co-ordination in dithiophosphinate complexes: $\Delta\nu$ = 50–70 for isobidentate ligands, 70–90 for anisobidentate ligands and > 90 cm^{-1} for monodentate complexes. The values for each of the thallium(III) dicyclohexyldithiophosphinate compounds are in agreement with the mode of co-ordination already assigned to them. In the diphenylthallium complex where the dithiophosphinate is isobidentate $\Delta\nu$ = 40 cm^{-1}, while an intermediate value of $\Delta\nu$ is found for the anisobidentate ligands in the monophenylthallium complex. In $[\mathrm{Tl}\{\mathrm{S_2P(C_6H_{11})_2}\}_3]$ the bands associated with the ν(P–S) vibration are broad, probably due to the presence of both types of ligand.

NMR Spectra.—Table 9 lists selected ^{1}H, ^{13}C, ^{31}P and ^{205}Tl NMR spectral data for the compounds synthesized and the free acid, all as solutions in CDCl$_3$. The ^{205}Tl chemical shifts and ^{1}H–^{205}Tl coupling constants confirm that protodemetallation has occurred, as discussed above. The chemical shift of the Tl^{III} nucleus appears to depend heavily on the number of metal-bound phenyl groups, the order for the dithiophosphinates being $\mathrm{TlPh_2}^{+}$ > TlPh^{2+} > Tl^{3+}. The above sequence may be extended to TlPh$_3$ (δ 3814 in Et$_2$O solution[25]), so that δ(^{205}Tl^{III}) values are in the order $\mathrm{TlPh_3}$ > $\mathrm{TlPh_2}^{+}$ > TlPh^{2+} > Tl^{3+} as phenyl groups are successively replaced by dithiophosphinate anions.

In both $[\mathrm{TlPh_2}\{\mathrm{S_2P(C_6H_{11})_2}\}]$ and $[\mathrm{TlPh}\{\mathrm{S_2P(C_6H_{11})_2}\}_2]$

Table 9 Selected NMR spectral data for the complexes in $CDCl_3$ solutions[a]

Compound	$\delta(^{31}P)$	$\delta(^{1}H)$[b]	$^{n}J(^{1}H-^{205}Tl)$	$\delta(^{13}C)$[b]	$^{n}J(^{13}C-^{205}Tl)$	$\delta(^{205}Tl)$
$HS(S)P(C_6H_{11})_2$	85.85 (s)	—	—	—	—	—
$[TlPh_2\{S_2P(C_6H_{11})_2\}]$	94.24 (s)	7.28 (d, H_o)	431.8	165.81 (d, C_i)	4259.2	3545s
				136.92 (d, C_o)	331.8	
				129.31 (d, C_m)	436.9	
				128.72 (d, C_p)	82.6	
$[TlPh\{S_2P(C_6H_{11})_2\}_2]$	91.76 (s)	7.85 (d, H_o)	796.4	159.71 (d, C_i)	7651.4	3302s
		7.50 (d, H_m)	283.8	134.10 (d, C_o)	459.1	
		7.35 (d, H_p)	116.0	129.19 (d, C_m)	788.4	
				129.14 (d, C_p)	164.1	
$[Tl\{S_2P(C_6H_{11})_2\}_3]\cdot CHCl_3$	98.58 (s)					2408q
	86.21 (s)					

[a] δ In ppm, *J* in Hz. [b] Signals for Ph groups; multiplicity, assignment in parentheses; d = doublet, q = quartet, s = singlet.

the ^{31}P nucleus is deshielded with respect to the free acid, as has been observed in dicyclohexyldithiophosphinates of other main-group metal or organometallic cations.[26] The absence of any $^{31}P-^{205}Tl$ coupling may be due to lability, which is usual in phosphorodithioate complexes.[27]

The ^{31}P NMR spectrum of $[Tl\{S_2P(C_6H_{11})_2\}_3]$ exhibits two signals at δ 98.6 and 86.2. The possibility that this complex may have undergone a redox reaction[18,19] in the course of recording the spectrum was ruled out; such a reaction would have led to signals for residual $[Tl\{S_2P(C_6H_{11})_2\}_3]$, for $[Tl\{S_2P(C_6H_{11})_2\}]$ and for $\{S_2P(C_6H_{11})_2\}_2$.* An alternative explanation for there being two signals due to P in the tris complex is that as the number of metal-bound phenyl groups decreases the effective charge of the $TlPh_n$ moiety increases; thus ligand-exchange slows down allowing detection of the P resonances of the isobidentate ligand, the other signal being attributable to the P atoms of the two anisobidentate ligands. Although the appearance of the thallium signal in the ^{205}Tl NMR spectrum [a quartet with $J = 439.4$ Hz, see Fig. 1(*a*)] suggests that the $^{2}J(^{205}Tl-^{31}P)$ couplings to the two types of P atom are very similar, the origin of the multiplicity of this signal must actually be more complex, since although the two phosphorus signals in the ^{31}P spectrum are rather broad they are not split by coupling to the thallium.

Acknowledgements

We thank the Xunta de Galicia (Spain) for financial support under Project XUGA 20302A94.

---

* A ^{31}P spectrum run immediately after addition of an excess of I_2 (12.6 mg, 0.10 mmol) to a solution of $[NEt_4][S_2P(C_6H_{11})_2]$ (7.7 mg, 0.03 mmol) in $CDCl_3$ gave a signal at δ 101.1 for $\{S_2P(C_6H_{11})_2\}_2$.

References

1 A. N. Pudovik, R. A. Cherkasov and I. V. Shergina, *J. Gen. Chem. USSR* (*Engl. Transl.*), 1971, **41**, 1477.
2 A. N. Pudovik, R. A. Cherkasov, I. V. Bykova, G. I. Evstaf'ev, Z. I. Zemskaya and M. N. Nazypov, *J. Gen. Chem. USSR* (*Engl. Trans.*), 1972, **42**, 76.
3 A. A. S. Elkhaldy, R. K. Mehrotra and G. Srivastava, *Synth. React. Inorg. Met.-Org. Chem.*, 1992, **22**, 997.
4 G. E. Coates and R. N. Mukherjee, *J. Chem. Soc.*, 1964, 1295.
5 I. F. Gun'kin, A. I. Idelevich and K. P. Butin, *Organomet. Chem. USSR*, 1990, **3**, 304.
6 Ch. Burschka, *Z. Anorg. Allg. Chem.*, 1982, **485**, 217.
7 B. Walther, *Z. Anorg. Allg. Chem.*, 1973, **395**, 112; U. Buadis and M. Wieber, *Z. Anorg. Allg. Chem.*, 1979, **448**, 79.
8 F. Bonati, S. Cenini and R. Ugo, *J. Organomet. Chem.*, 1967, **9**, 395.
9 N. Walker and D. Stuart, *Acta Crystallogr., Sect. A*, 1983, **38**, 158.
10 G. M. Sheldrick, SHELX 76, A Program for crystal structure determination, University of Cambridge, 1976; G. M. Sheldrick, SHELXS 86, A Program for the Solution of Crystal Structures from X-ray Diffraction Data, University of Göttingen, 1986.
11 B. A. Frenz, *The Enraf-Nonius CAD4 SDP in Computing in Crystallography*, Delft University Press, Delft, 1985.
12 C. K. Johnson, ORTEP, Report ORNL-3794, Oak Ridge National Laboratory, TN, 1965.
13 E. Keller, SCHAKAL, A Program for Plotting Molecular and Crystal Structures, University of Freiburg, 1988.
14 D. T. Cromer and J. B. Mann, *Acta Crystallogr., Sect. A*, 1968, **24**, 321.
15 D. T. Cromer and D. J. Liberman, *J. Chem. Phys.*, 1970, **533**, 1891.
16 *International Tables for X-Ray Crystallography*, Kynoch Press, Birmingham, 1974, vol. 4.
17 A. McKillop, J. D. Hunt and E. C. Taylor, *J. Organomet. Chem.*, 1970, **24**, 77.
18 W. Kuchen and H. Mayatepeck, *Chem. Ber.*, 1968, **101**, 3454.
19 S. Esperas and S. Husebye, *Acta Chem. Scand., Ser. A*, 1974, **28**, 1015.
20 I. Haiduc, *Rev. Inorg. Chem.*, 1981, **3**, 353.
21 R. T. Griffin, K. Henrick, R. W. Matthews and M. McPartlin, *J. Chem. Soc., Dalton Trans.*, 1980, 1550.
22 A. Bondi, *J. Phys. Chem.*, 1964, **68**, 441.
23 H. Abrahanson, J. R. Heinan and L. Pignolet, *Inorg. Chem.*, 1975, **14**, 2070.
24 I. Haiduc, I. Silaghi-Dumitrescu, R. Grecu, R. Constantinescu and L. Silaghi-Dumitrescu, *J. Mol. Struct.*, 1984, **114**, 467.
25 J. F. Hinton, K. R. Metz and R. W. Briggs, *Prog. Nucl. Magn. Reson. Spectrosc.*, 1988, **20**, 423.
26 J. S. Casas, M. S. García-Tasende, A. Sánchez, J. Sordo, E. M. Vázquez-López, E. E. Castellano and J. Zukerman-Schpector, *Inorg. Chim. Acta*, 1993, **209**, 137; J. S. Casas, A. Castiñeiras, A. Sánchez, J. Sordo and E. M. Vázquez-López, *J. Organomet. Chem.*, 1994, **468**, 1.
27 A. M. Bond, R. Cotton, D. Dakternieks, M. L. Dillon, J. Hannenstein and J. Moir, *Aust. J. Chem.*, 1981, **34**, 1393.

Received 13*th November* 1994; *Paper* 4/06275B